Interplay between local dynamics and mechanical reinforcement in glassy polymer nanocomposites

Adam P. Holt,[1,*,†] Vera Bocharova,[2,‡] Shiwang Cheng,[2] Alexander M. Kisliuk,[2] Georg Ehlers,[3] Eugene Mamontov,[4] Vladimir N. Novikov,[5] and Alexei P. Sokolov[1,2,5]

[1]*Department of Physics and Astronomy, University of Tennessee, Knoxville, Tennessee 37996, USA*
[2]*Chemical Sciences Division, Oak Ridge National Laboratory Oak Ridge, Tennessee 37831, USA*
[3]*Quantum Condensed Matter Division, Oak Ridge National Laboratory, Oak Ridge, Tennessee 37831, USA*
[4]*Chemical & Engineering Materials Division, Oak Ridge National Laboratory, Oak Ridge, Tennessee 37831, USA*
[5]*Department of Chemistry, University of Tennessee, Knoxville, Tennessee 37996, USA*

The modification of polymer dynamics in the presence of strongly interacting nanoparticles has been shown to significantly change the macroscopic properties above the glass transition temperature of polymer nanocomposites (PNCs). However, much less attention has been paid to changes in the dynamics of glassy PNCs. Analysis of neutron and light scattering data presented herein reveals a surprising enhancement of local dynamics, e.g., fast picosecond and secondary relaxations, in glassy PNCs accompanied with a strengthening of mechanical modulus. We ascribe this counter-intuitive behavior to the complex interplay between chain packing and stretching within the interfacial layer formed at the polymer-nanoparticle interface.

For the past decade, the augmentation of segmental and chain dynamics *via* the addition of nanoparticles (NPs) with strong polymer-NP interactions has been actively studied with the aim of tailoring the material properties of polymer nanocomposites (PNCs) [1–14]. Many studies using NMR, dielectric spectroscopy, neutron scattering, and other techniques revealed significant changes in segmental dynamics for the adsorbed polymers chains in the interfacial layer at the polymer-NP interface [15,16]. At temperatures above the glass transition temperature (T_g), it has been also demonstrated that the polymer within the interfacial region possesses stronger mechanical properties than the neat polymer, which ultimately leads to the improvement of properties of the entire composite. However, within the nonequilibrium glassy state, this expectation may not hold true [17,18], especially considering that the mechanical properties of glassy polymers are largely determined by dynamical processes faster than segmental motions, that is, local processes such as secondary relaxations and fast picosecond dynamics [19–25].

Despite the vested interest in the segmental dynamics of PNCs, the details of which are extremely important for many applications such as mass [26] or ion transport [27], thermal processing [28], or reinforcement of rubbery materials [29], there has been little work concerning the modification of more localized dynamic processes such as β relaxations, γ relaxations, and the fast picosecond dynamics. Ding *et al.*, previously demonstrated that the addition of NPs can affect several time scales of polymer dynamics in different ways: frustrated molecular packing in PNCs leads to a softening of the material and speeding up of the secondary relaxations within the glassy state, while simultaneously increasing fragility and T_g (suppression of segmental dynamics) [30]. There is now a better understanding of these effects, for exam-

ple, Roh *et al.*, found larger stretching of segmental dynamics in neutron scattering spectra of 1,4-polybutadiene/carbon black nanocomposites emphasizing a broader distribution of relaxation times associated with a heterogeneous structure [31,32]. Furthermore, it was recently found that the local packing of segments in several model PNC systems depends strongly on the molecular weight of the matrix—an effect that should alter several different time scales of polymer dynamics at the polymer-NP interface [33]. Indeed, these effects were recently highlighted by Casalini and Roland studying the dynamics of extracted silica nanoparticles with absorbed poly(propylene glycol) chains obtained *via* solvent processing where they demonstrated that the polymer chains absorbed on the extracted NPs were much less dense and exhibited faster segmental and chain dynamics despite being physically tethered to the NP [34]. However, more recently, Tyagi *et al.*, measured the temperature dependence of the mean square displacement (MSD) of the same extracted NPs and found that the amplitude of the MSD was suppressed at temperatures above and below T_g—which one would expect for an increase in the local density [35]. Recent theoretical and experimental studies also suggested the importance of chain stretching in the interfacial layer for changes in segmental dynamics and mechanical properties of PNCs [18,36–38]. All these results suggest that the competition between interfacial interactions, chain packing, and stretching effects strongly influence the macroscopic properties of PNC, and a clear understanding of the interplay between these competing effects is required for the rational design of PNC with desirable properties.

In this Rapid Communication, we investigate the differences in the local dynamics and macroscopic mechanical properties of poly(2-vinylpyridine) (P2VP)/silica nanocomposites (PNCs) and P2VP-grafted-to-silica NPs (PGNs) in their glassy state by quasi-elastic neutron scattering, Brillouin light scattering (BLS), and broadband dielectric spectroscopy (BDS). These chemically similar materials were selected because they show significant difference in the interfacial segmental dynamics [38]. Our results reveal that the local dynamics in PNCs and PGNs are controlled primarily by the

---

*adam.holt.ctr@nrl.navy.mil
†Present Address: Naval Research Laboratory, Chemistry Division, Code 6100, Washington, DC 20375–5342, USA.
‡bocharovav@ornl.gov

changes in density, while the glassy mechanical properties such as the high frequency bulk and shear moduli are strongly affected by both, chain packing and chain stretching.

A detailed preparation of materials is presented in Ref. [38]. For all samples, the molecular weight of P2VP is 18 kg/mol, which is just about the entanglement molecular weight, $M_e = 17$ kg/mol [39]. For the PNC and PGN systems, spherical silica NPs with a diameter between 20–25 nm were synthesized following the modified Stöber method and prepared at nearly identical silica concentrations (PNC: 52 wt%, PGN: 49 wt%). Whereas the PNC system was mixed with the silica NPs, the PGN system has chains grafted from the surface of the NPs ($\sigma = 0.3$ chains/nm^2). The secondary relaxation of P2VP was characterized by BDS using a Novocontrol Alpha Analyzer (between 10^{-1} to 10^7 Hz) with a Quatro Cryosystem temperature controller (± 0.1 K). To determine the longitudinal and transverse sound velocities in the composite materials, BLS measurements were conducted at room temperature ($T = 293$ K) and spectra from both vertical-vertical and vertical-horizontal polarized light were collected from polymer films deposited onto silicon substrates in a combination of backscattering with ΘA scattering (RIΘA scattering, $\Theta = 90°$, $\lambda = 532$ nm, and $P = 100$ mW). The RIΘA scattering geometry allows compensation of the refractive index [40]. As a result, one can estimate the sound velocities without knowledge of the refractive index, for details see Ref. [41]. The mass densities of the composites were determined *via* a gas pycnometer (Micromeretics Accupyc II 1340) at room temperature ($T = 293$ K). Additional details can be found in references 15 and 30. Neutron scattering spectra were measured at Spallation Neutron Source (ORNL) with both the Cold Neutron Chopper Spectrometer (CNCS) and Backscattering Spectrometer (BASIS) [42–43]. Powder samples were placed in aluminum cans and measured at $T = 300$ K. For CNCS, the incident neutron energy was 3.32 meV and the presented spectra were summed over a Q range of $0.2-1.5$ Å^{-1}. The wavelength center of the incident bandwidth for BASIS measurements was 6.15 Å, the measured energy range of -0.1 to 0.5 meV and the spectra were summed over all Q values [$0.2-2$ Å^{-1}]. All spectra were corrected using a vanadium standard and an empty can using the DAVE software package. No multiple scattering corrections were applied. To minimize physical aging effects, samples were annealed at 473 K and cooled to the measurement temperatures at 5 K/min prior to all experimental measurements ($\geqslant 70$ K below T_g).

Figure 1(a) presents the dielectric loss spectra of the materials well below T_g ($T_g^{\text{dielectric}} = 362$ K) to illustrate the secondary β relaxation of P2VP and its changes with the addition of nanoparticles or grafting from the surface. While there is negligible effect on the low-frequency tail of the peak, the high frequency wing is broadened in a similar fashion for the case of both PNC and PGN systems. The quantitative changes in the dielectric spectra can be captured by fitting the dielectric loss to the Havriliak-Negami (HN) function:

$$\varepsilon''(\omega) = -\text{Im}[\Delta\varepsilon/(1 + (i\omega\tau_{\text{HN}})^\alpha)^\gamma],$$

where $\Delta\varepsilon$ is the dielectric strength of the relaxation process, τ_{HN} is the HN relaxation time, and the exponents α and γ describe the symmetric and asymmetry broadening of
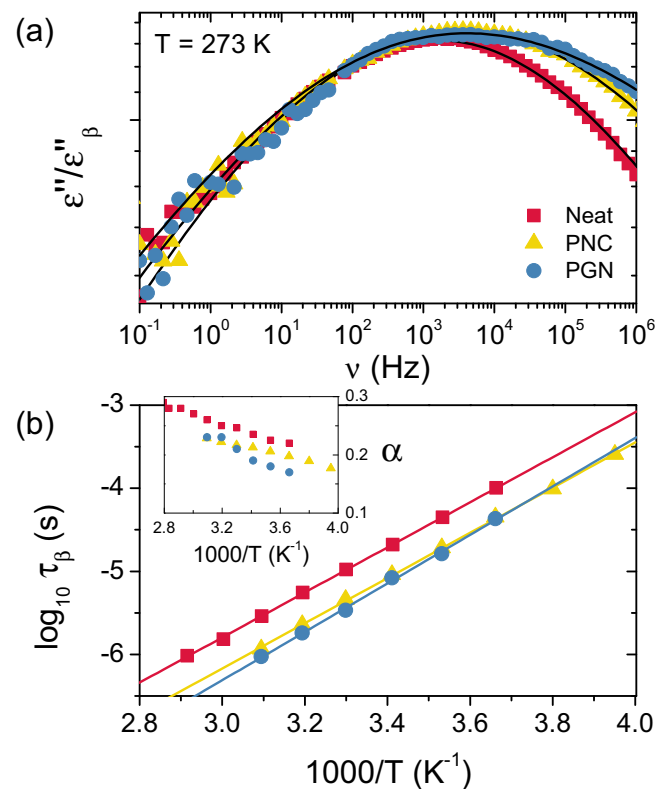

FIG. 1. (a) Normalized dielectric loss spectra well below the glass transition temperature illustrating the pronounced secondary, β-relaxation process of neat P2VP, P2VP-silica nanocomposite (PNC), and P2VP-grafted-to-silica (PGN). Solid black lines are HN fits. (b) The temperature dependence of the respective β-relaxations with Arrhenius fits (lines). Inset: Temperature dependence of the symmetric stretching parameter α, from the HN fitting function.

the spectra, respectively. The τ_{HN} is related to the maximum of the β relaxation by the following relation $\tau_\beta = \tau_{\text{HN}}[\sin(\pi\gamma/2(\alpha+1))/\sin(\pi\gamma\alpha/2(\alpha+1))]^\gamma$.

The β-relaxation process in PNC and PGN appears half an order of magnitude faster than in the neat polymer [Fig. 1(b)]. The molecular nature of the β relaxation in P2VP is closely related to the rotational reorientation of pyridine side groups with a previously reported Arrhenius activation energy of 53 kJ/mol [44]. Our analysis [Fig. 1(b)] revealed the energy barrier of 52 kJ/mol for the neat and PNC samples, and 55 kJ/mol for PGN. The spectrum of the β relaxation also broadens, as quantified by the symmetric HN stretching parameter α [inset of Fig. 1(b)], indicating a broader distribution of relaxations times. The fit also reveals the asymmetry parameter γ to be ~ 1.0 for all samples at all temperatures.

Figure 2 presents neutron scattering data as the susceptibility spectra: $\chi''(\upsilon) = I(\upsilon)/[n(\upsilon)]$, where $I(\upsilon)$ is the incoherent dynamic structure factor summed over all measured Q values, and $n(\upsilon) = [\exp(\hbar\omega/k_BT) - 1]^{-1}$ is the Bose factor. Figure 2 combines the dynamic range of both CNCS and BASIS to cover a large dynamic range of the fast dynamics within our systems. At high frequency ($\sim 10^3$ GHz), the microscopic peak of the neat, PNC, and PGN appears unaltered. However, a significant increase in the quasielastic intensity appears at
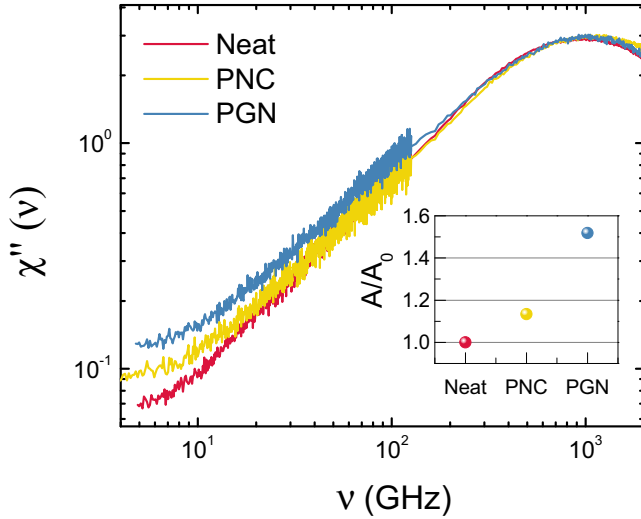
FIG. 2. Neutron scattering susceptibility spectra ($T = 300$ K, summed over all Q values, combined BASIS and CNCS measurements) normalized at the microscopic peak. Inset: the normalized area (A/A_0) under the curve of the fast dynamics contribution to the spectrum for each sample (approximately 4–30 GHz), where A_0 is the integrated intensity for the neat polymer.

frequencies below ∼100 GHz, with the largest increase observed for PGN (Fig. 2). The intensity of this quasielastic scattering reflects the amplitude of the fast picosecond fluctuations traditionally ascribed to a rattling in a cage". The increase in the amplitude of the fast dynamics indicates an increase in the mean squared displacement of hydrogen atoms which would be expected for a material with higher free volume (or lower density). Interestingly, the PGN system, which exhibits the largest increase in the amplitude of the fast dynamics, also has the largest increase in T_g and the strongest suppression of segmental dynamics, despite the highest amount of apparent free volume among the three samples [38].

The measured mass densities are 1.152 ± 0.008, 1.584 ± 0.006, and 1.476 ± 0.005 g/cm^3 for the neat polymer, PNC, and PGN, respectively, with an error of 1%. Assuming volume additivity, $\overline{\rho}_{\text{matrix}} = \frac{\rho_{\text{PNC}} - \rho_{\text{NP}}\phi_{\text{NP}}}{1 - \phi_{\text{NP}}}$ (here ρ_{PNC} and ρ_{NP} are the densities of the PNC or PGN and NPs, respectively, and ϕ_{NP} is the volume fraction of NPs), and taking $\rho_{\text{NP}} = 2.405 \pm 0.002$ g/cm^3, we estimate the average density of the polymer matrix, $\overline{\rho}_{\text{matrix}}$, to be 1.157 g/cm^3 in PNC and 1.077 g/cm^3 in PGN. Details of the density analysis have been presented in Ref. [30]. It appears that the averaged matrix density of the PNC is almost identical ($< 0.65\%$ and within error) to that of the neat polymer, while the matrix density in the PGN is 7% lower (Table I).

Figure 3(a) presents the BLS spectra with the longitudinal modes (LM) in the main figure and transverse modes (TM) in the inset. At a scattering angle of 90°, we observe single phonons for both modes, consistent with results for annealed P2VP films in Ref. [14]. To extract the longitudinal and transverse sound frequencies, we fit our data to the damped harmonic oscillator model:

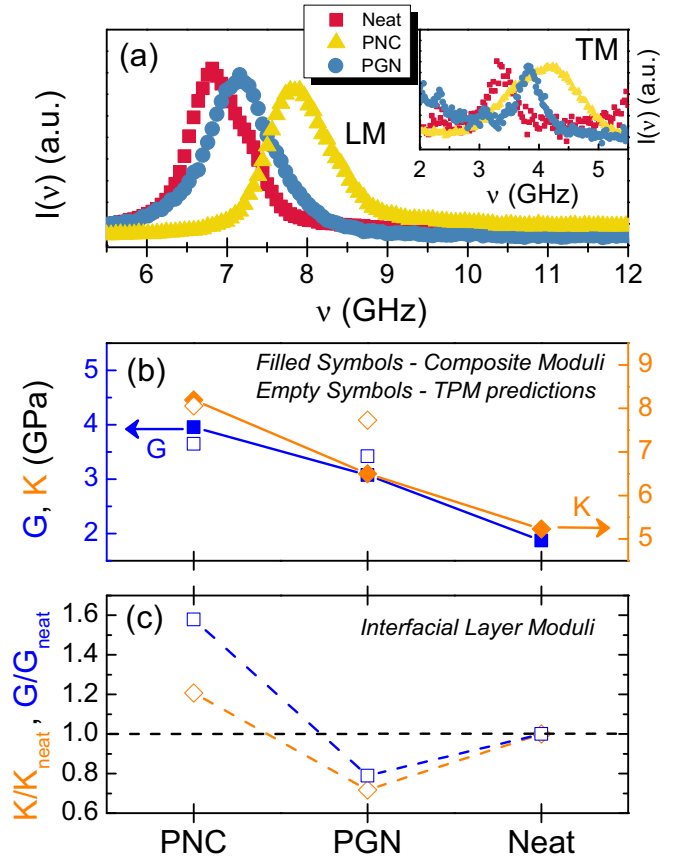$$I(v) = \frac{\Gamma I_0}{(v^2 - v_{L,T}^2) + \Gamma^2} + B,$$

FIG. 3. (a) A representative plot of the longitudinal mode (LM) from Brillouin light scattering of neat P2VP, P2VP-silica nanocomposite (PNC), and P2VP-grafted-to-silica (PGN). Inset: transverse mode (TM) from depolarized light scattering. (b) The composite shear modulus (G), and bulk modulus (K) for each material compared to predictions from the two-phase model (using ILM and assuming $\phi_l \to 0$). (c) The relative effective moduli of the polymer matrix from ILM calculations.

where I_0 is the peak intensity, Γ is a damping factor, $v_{L,T}$ is the peak position, and B is the background. Using the frequencies of the BLS peaks, we estimate the longitudinal and transverse sound velocities using the linear dispersion relationship for acoustic modes: $V_{L,T} = 2\pi v_{L,T}/Q$, where $Q = 2\pi \sqrt{2}/\lambda_{\text{laser}}$ (for RIΘA scattering at 90°). The longitudinal modulus ($M = \rho V_L^2$), shear modulus ($G = \rho V_T^2$), and bulk modulus ($K = M - 4/3G$) of the composites were computed by using the mass density (ρ_{PNC}) of the composite measured by pycnometry. The mechanical moduli for the composites and matrix are presented in Fig. 3(b). The PNC system exhibits the strongest increase in mechanical moduli while the PGN system shows a relatively weaker enhancement when compared to a neat polymer. To understand these data, we directly compare our results to the prediction from the two-phase model (TPM). This model was selected based on our previous work where we demonstrated that the TPM can better predict the mechanical properties than the Wood's law, which originates from a simple mixing rule [33]. For the TPM, we assume that the polymer matrix has the same modulus as the neat polymer [45,46]. The data from TPM model are presented

TABLE I. Mechanical properties from Brillouin light scattering and pycnometry and for the interfacial layer calculated from the interfacial layer model (ILM).

Sample	V_L (m/s)	V_T (m/s)	ρ_{PNC} (kg/m^3)	ρ_{matrix} (kg/m^3)	M_{comp} (GPa)	M_{int} (GPa)	G_{comp} (GPa)	G_{int} (GPa)	K_{comp} (GPa)	K_{int} (GPa)	T_g[a] (K)
Neat	2603	1275	1152	1152	7.8	n/a	1.9	n/a	5.3	n/a	367.9
PNC	2983	1633	1584	1157	14.1	10.4	4.2	3.0	8.5	5.5	371.1
PGN	2709	1452	1476	1077	10.5	5.8	3.0	1.5	6.5	4.3	377.0

[a]Values from Ref. [38].

in Fig. 3(b) as empty symbols. The differences between the experiments and the TPM model predictions are noticeable for both PNC and PGN. Interestingly, for the PGN, the experimental data falls below the prediction of the TPM model while the opposite is true in the case of the PNC. These results indicate that the matrix moduli are different than that of the neat polymer.

In our previous detailed BLS studies, we have demonstrated that the individual contribution of the interfacial layer to the mechanical properties of PNCs could be well-described by the interfacial layer model (ILM) at all nanoparticle loadings (see Ref. [41] for details) [18]. The validity of the ILM model results was also confirmed by the finite element analysis in Ref. [18] as well. We now utilize the ILM to calculate the bulk and shear moduli of interfacial layer. The results [Fig. 3(c), Table I] reveal a significant increase in the interfacial layer moduli in the case of PNC, while strong drop in the moduli is observed in PGN. Clearly, the differences between the interfacial layer moduli for the PNC and PGN are likely due to the drastically different structural organization of interfacial layers in these systems.

The presented results combined with earlier studies of segmental dynamics reveal a surprising and counterintuitive picture: while the strongest suppression of segmental dynamics and the largest increase in T_g is observed in the PGN samples, this system exhibits the smallest change in the mechanical moduli combined with the largest enhancement of the fast dynamics and decrease in density (Table I). These findings demonstrate that the strong suppression of the segmental dynamics does not necessarily lead to stronger mechanical reinforcement, at least in these two systems. Moreover, polymer dynamics on different time scales can be affected in very different ways. While the strongest suppression of the segmental dynamics appears in the PGN, the strongest enhancement of mechanical modulus appears in PNC. At the same time the secondary relaxation is similar in the PGN and PNC and is faster than in neat polymer, while enhancement of the fast dynamics is the strongest in the PGN. We emphasize that earlier studies revealed a stronger chain stretching in the interfacial layer of PGN in comparison with that in PNC [38]. Thus, the way polymer chains are attached to the nanoparticles in composite materials significantly affects frustration in chain packing (density) and stretching. This has different effects on fast dynamics and secondary relaxation, segmental dynamics, and mechanical properties in the glassy state.

A theory developed for thin polymer brushes on a substrate suggests that chain stretching in the interfacial layer might be one of the major mechanisms leading to suppression of segmental dynamics [36]. The concept of anisotropic segmental stretching at the polymer-nanoparticle interface was proposed as the main mechanism of the suppression of segmental dynamics in PNCs and PGNs [38]. Apparently, the density changes play a weaker role than the chain stretching in the suppression of segmental dynamics and increase in T_g. At the same time, changes in density strongly affect the amplitude of the fast picosecond fluctuations (rattling in a cage), while chain stretching apparently does not play significant role in the fast dynamics. Therefore we conclude that there is a delicate interplay between chain stretching and density effects in the interfacial region of nanocomposite materials; where the effect of stretching slows down the segmental dynamics and leads to an increase in the local T_g, while changes in density influences the faster dynamics. At the same time, the change in density of the interfacial layer in PGN leads to a decrease in its mechanical properties, despite chain stretching. The latter leads to strong increase in the mechanical properties of PNC where density remains essentially the same as in the neat polymer.

In summary, our studies of glassy PNC and PGN systems of identical MW and silica content revealed a surprising difference in their properties below T_g: while strongest suppression of the segmental dynamics is observed in PGN, it also exhibits the strongest enhancement of the fast dynamics and secondary relaxation, at the same time PNC shows significantly larger strengthening of mechanical properties than PGN. Interestingly, PGN having lower density exhibits a higher T_g. These results contradict the traditional density scaling of segmental dynamics in polymers [47] and suggest a convolution between multiple effects (i.e., density and chain stretching). Additionally, the effect of density changes also influences the macroscopic mechanical properties of these materials where the shear and bulk moduli of the matrix are both higher in PNC than in the neat polymer but are lower in PGN. As a result, a detailed analysis by the ILM reveals that the moduli of the interfacial layer in PNC and PGN systems differ noticeably. These results demonstrate that one can control segmental, faster dynamics, and mechanical strength of composite materials by tuning two independent variables—chain stretching and local density at the interfacial layer surrounding nanoparticles. This discovery might be important for design of composite materials with desired macroscopic properties.

[1] S. Cheng, B. Carroll, V. Bocharova, J.-M. Carrillo, B. G. Sumpter, and A. P. Sokolov, Focus: Structure and dynamics of the interfacial layer in polymer nanocomposites with attractive interactions, J. Chem. Phys. **146**, 203201 (2017).

[2] L. Schadler, Nanocomposites: Model interfaces, Nat. Mater. **6**, 257 (2007)

[3] J. Moll, and S. K. Kumar, Glass transitions in highly attractive highly filled polymer nanocomposites, Macromolecules **45**, 1131 (2012).

[4] N. Jouault, J. F. Moll, D. Meng, K. Windsor, S. Ramcharan, C. Kearney, and S. K. Kumar, Bound polymer layer in nanocomposites, ACS Macro Lett. **2**, 371 (2013).

[5] A. Bansal, H. Yang, C. Li, K. Cho, B. C. Benicewicz, S. K. Kumar, and L. S. Schadler, Quantitative equivalence between polymer nanocomposites and thin polymer films, Nat. Mater. **4**, 693 (2005).

[6] Y. Huang and D. R. Paul, Effect of molecularweight and temperature on physical aging of thinglassy poly(2,6-dimethyl-1,4-phenylene oxide) films, J. Polym. Sci. Part B Polym. Phys. **45**, 1390 (2007).

[7] F. W. Starr, T. B. Schrøder, and S. C. Glotzer, Molecular dynamics simulation of a polymer melt with a nanoscopic particle, Macromolecules **35**, 4481 (2002).

[8] F. W. Starr and J. F. Douglas, Modifying Fragility and Collective Motion in Polymer Melts with Nanoparticles, Phys. Rev. Lett. **106**, 115702 (2011).

[9] J. M. Kropka, V. G. Sakai, and P. F. Green, Local polymer dynamics in polymer - C 60 mixtures, Nano Lett. **8**, 1061 (2008).

[10] D. Fragiadakis, L. Bokobza, and P. Pissis, Dynamics near the filler surface in natural rubber-silica nanocomposites, Polymer **52**, 3175 (2011).

[11] D. Fragiadakis, P. Pissis, and L. Bokobza, Modified chain dynamics in poly(dimethylsiloxane)/silica nanocomposites, J. Non. Cryst. Solids **352**, 4969 (2006).

[12] P. B. A. Betancourt, J. F. Douglas, and F. W. Starr, Fragility and cooperative motion in a glass-forming polymer-nanoparticle composite, Soft Matter **9**, 241 (2013).

[13] P. Voudouris, J. Choi, N. Gomopoulos, R. Sainidou, H. Dong, K. Matyjaszewski, M. R. Bockstaller, and G. Fytas, Anisotropic elasticity of quasi-one-component polymer nanocomposites, ACS Nano **5**, 5746 (2011).

[14] D. Zhao, D. Schneider, G. Fytas, and S. K. Kumar, Controlling the thermomechanical behavior of nanoparticle/polymer films, ACS Nano **8**, 8163 (2014).

[15] P. Rittigstein, R. D. Priestley, L. J. Broadbelt, and J. M. Torkelson, Model polymer nanocomposites provide an understanding of confinement effects in real nanocomposites, Nat. Mater. **6**, 278 (2007).

[16] P. Rittigstein and J. M. Torkelson, Polymer–nanoparticle interfacial interactions in polymer nanocomposites: Confinement effects on glass transition temperature and suppression of physical aging, J. Polym. Sci., Part B Polym. Phys. **44**, 2935 (2006).

[17] D. Maillard, S. K. Kumar, B. Fragneaud, J. W. Kysar, A. Rungta, B. C. Benicewicz, H. Deng, L. C. Brinson, and J. F. Douglas, Mechanical properties of thin glassy polymer films filled with spherical polymer-grafted nanoparticles, Nano Lett. **12**, 3909 (2012).

[18] S. Cheng, V. Bocharova, A. Belianinov, S. Xiong, A. M. Kisliuk, S. Somnath, A. P. Holt, O. S. Ovchinnikova, S. Jesse, H. Martin, T. Etampawala, M. D. Dadmun, and A. P. Sokolov, Unraveling the mechanism of nanoscale mechanical reinforcement in glassy polymer nanocomposites, Nano Lett. **16**, 3630 (2016).

[19] C. J. T. Landry and P. M. Henrichs, The influence of blending on the local motions of polymers: Studies involving polycarbonate, poly(methyl methacrylate), and a polyester, Macromolecules **22**, 2157 (1989).

[20] K. L. Ngai, R. W. Rendell and A. F. Yee, Local molecular motions in glassy and dissolved polycarbonates, Macromolecules **21**, 3396 (1988).

[21] A. D. Mulliken and M. C. Boyce, Mechanics of the rate-dependent elastic–plastic deformation of glassy polymers from low to high strain rates, Int. J. Solids Struct. **43**, 1331 (2006).

[22] K. L. Ngai, R. W. Rendell, A. F. Yee, and D. J. Plazek, Plasticized glassy polycarbonates, Macromolecules, **24**, 61 (1991).

[23] C. Xiao, J. Y. Jho, A. F. Yee, and A. Arbor, Correlation between the shear yielding behavior and secondary relaxations of bisphenol a polycarbonate and related copolymers, Macromolecules, **27**, 2761 (1994).

[24] F. J. Hörth, K. J. Kuhn, J. Mertes, and G. P. Hellmann, On the mechanical γ-relaxation modes of polycarbonate, Polymer **33**, 1223 (1992).

[25] J Heijboer. Dynamic mechanical properties of amorphous polymers, in *Static and Dynamic Properties of the Polymeric Solid State*, edited by R. A. Pethrick and R. W. Richards, Proceedings of the NATO Advanced Study Institute (Springer, Netherlands: Dordrecht, 1982), pp. 197–211.

[26] N. C. Su, Z. P. Smith, B. D. Freeman, and J. J. Urban, Size-dependent permeability deviations from maxwells model in hybrid cross-linked poly(ethylene glycol)/silica nanoparticle membranes, Chem. Mater. **27**, 2421 (2015).

[27] F. Fan, W. Wang, A. P. Holt, H. Feng, D. Uhrig, X. Lu, T. Hong, Y. Wang, N.-G. Kang, J. Mays, and A. P. Sokolov,

Effect of molecular weight on the ion transport mechanism in polymerized ionic liquids, Macromolecules **49**, 4557 (2016).

[28] J. Jordan, K. I. Jacob, R. Tannenbaum, M. A. Sharaf, and I. Jasiuk, Experimental trends in polymer nanocomposites—a review, Mater. Sci. Eng. A **393**, 1 (2005).

[29] A. Mujtaba, M. Keller, S. Ilisch, H. J. Radusch, M. Beiner, T. Thurn-Albrecht, and K. Saalwächter, Detection of surface-immobilized components and their role in viscoelastic reinforcement of rubber-silica nanocomposites, ACS Macro Lett. **3**, 481 (2014).

[30] Y. Ding, S. Pawlus, A. P. Sokolov, J. F. Douglas, A. Karim, and C. L. Soles, Dielectric spectroscopy investigation of relaxation in C60−polyisoprene nanocomposites, Macromolecules **42**, 3201 (2009).

[31] J. H. Roh, M. Tyagi, T. E. Hogan, and C. M. Roland, Space-dependent dynamics in 1,4-polybutadiene nanocomposite, Macromolecules **46**, 6667 (2013).

[32] J. H. Roh, M. Tyagi, T. E. Hogan, and C. M. Roland, Effect of binding to carbon black on the dynamics of 1,4-polybutadiene, J. Chem. Phys. **139**, 134905 (2013).

[33] S. Cheng, A. P. Holt, H. Wang, F. Fan, V. Bocharova, H. Martin, T. Etampawala, B. T. White, T. Saito, N.-G. Kang, M. D. Dadmun, J. W. Mays, and A. P. Sokolov, Unexpected Molecular Weight Effect in Polymer Nanocomposites, Phys. Rev. Lett. **116**, 038302 (2016).

[34] R. Casalini and C. M. Roland, Local and global dynamics in polypropylene glycol/silica composites, Macromolecules **49**, 3919 (2016).

[35] M. Tyagi, R. Casalini, and C. M. Roland, Short time and structural dynamics in polypropylene glycol nanocomposite, Rubber Chem. Technol. **90**, 264 (2017).

[36] F. T. Oyerokun and K. S. Schweizer, Theory of glassy dynamics in conformationally anisotropic polymer systems, J. Chem. Phys. **123**, 224901 (2005).

[37] S. A Kim, R. Mangal, and L. A. Archer, Relaxation dynamics of nanoparticle-tethered polymer chains, Macromolecules **48**, 6280 (2015).

[38] A. P. Holt, V. Bocharova, S. Cheng, A. M. Kisliuk, B. T. White, T. Saito, D. Uhrig, J. P. Mahalik, R. Kumar, A. E. Imel, T. Etampawala, H. Martin, N. Sikes, B. G. Sumpter, M. D. Dadmun, and A. P. Sokolov, Controlling interfacial dynamics: Covalent bonding versus physical adsorption in polymer nanocomposites, ACS Nano **10**, 6843 (2016).

[39] C.-T. Lo and K.-H. Tsui, The dispersion of magnetic nanorods in poly(2-vinylpyridine), Polym. Int. **62** (2013).

[40] J. K. Krüger, J. Embs, J. Brierley, and R. A Jiménez, New brillouin scattering technique for the investigation of acoustic and opto-acoustic properties: Application to polymers, J. Phys. D. Appl. Phys. **31**, 1913 (1998).

[41] See Supplemental Material at http://link.aps.org/supplemental/10.1103/PhysRevMaterials.1.062601 for a detailed description of the interfacial layer model.

[42] G. Ehlers, A. A. Podlesnyak, and A. I. Kolesnikov, The cold neutron chopper spectrometer at the spallation neutron source: A review of the first 8 years of operation, Rev. Sci. Instrum. **87**, 93902 (2016).

[43] E. Mamontov and K. W. A Herwig, Time-of-flight backscattering spectrometer at the spallation neutron source, BASIS, Rev. Sci. Instrum. **82**, 85109 (2011).

[44] P. Papadopoulos, D. Peristeraki, G. Floudas, G. Koutalas, and N. Hadjichristidis, Origin of glass transition of poly(2-vinylpyridine). A temperature- and pressure-dependent dielectric spectroscopy study, Macromolecules **37**, 8116 (2004).

[45] M. E. McConney, S. Singamaneni, and V. V. Tsukruk, Probing soft matter with the atomic force microscopies: Imaging and force spectroscopy, Polym. Rev. **50**, 235 (2010).

[46] M. Qu, F. Deng, S. M. Kalkhoran, A. Gouldstone, A. Robisson, and K. J. Van Vliet, Nanoscale visualization and multiscale mechanical implications of bound rubber interphases in rubber–carbon black nanocomposites, Soft Matter **7**, 1066 (2011).

[47] C. M. Roland, Relaxation phenomena in vitrifying polymers and molecular liquids, Macromolecules **43**, 7875 (2010).